Clays and Clay Minerals, Vol. 45, No. 3, 404–417, 1997.

CRYSTALLOGRAPHIC CONTROLS ON THE ALTERATION OF MICROCLINE PERTHITES FROM THE SPRUCE PINE DISTRICT, NORTH CAROLINA

JULIA M. SHEETS† AND RODNEY T. TETTENHORST

Department of Geological Sciences, Ohio State University, Columbus, Ohio 43210-1110

Abstract—Altered perthites from a weathered pegmatite in the Spruce Pine District, North Carolina, were characterized by electron microprobe as a K-rich microcline host with lesser Na-rich plagioclase having a lamellar morphology. Light-optical and transmission electron microscopy (TEM) show microtextural elements such as phase boundaries, holes and microfractures that could serve as potential nucleation sites for alteration to clay minerals.

The host microcline contains albite and pericline twinning textures that vary in character; the amount of each twinning type and/or the size of twin individuals changes on a μm scale. Plagioclase ranges from large lamellar vein and film albite (visible in the light microscope) to cryptoperthite whose size ranges from μm to perhaps 100 Å. The smallest-scale albite appears to be a late-stage phase of exsolution in which lamellae have nucleated heterogeneously on albite-twin composition planes in the microcline.

Alteration is concentrated in vein and film albite, especially along grain boundaries with microcline. Powder X-ray diffraction (XRD) patterns of intensely altered pegmatite show halloysite. Holes, microfractures, vein albite/host microcline boundaries and microcline/halloysite boundaries trend parallel to the traces of (010) and {110}, suggesting that these directions are pathways along which fluids migrate. Cleavage and microfractures occur along, and holes are bounded by, these directions. Holes are associated with dislocations and the latter are observed at feldspar/clay boundaries. Twin domains and cryptoperthitic albite are less susceptible to alteration than coarse lamellar albite and regions containing negative crystals and microfractures. However, microtextures in some areas containing halloysite suggest that once fluids penetrate the crystal, alteration may proceed preferentially in more strongly twinned regions.

Key Words—Albite, Alteration, Crystallographic Control, Defects, Halloysite, Holes, Microcline, Microfractures, Microtextural Elements, Perthite, Phase Boundaries, Twinning.

INTRODUCTION

Understanding the mechanisms of alteration of feldspars to clay minerals under conditions at or near the earth's surface is essential for geochemical studies involving these minerals. In particular, previous studies suggest that specific microtextural elements within single crystals of the parent material are relatively more susceptible to alteration, and may influence the rate at which feldspar alters to clay.

A dissolution/reprecipitation mechanism for chemical weathering of feldspar is well established, and the transformation of feldspar to clay is nontopotactic (Eggleton 1986). However, the influence of parent mineral microstructure on dissolution and reprecipitation during alteration of feldspar to clay is not well understood. Defects in parent feldspars may be important early in the alteration of feldspars to clays, but less important at more advanced stages of the transformation (Eggleton and Buseck 1980: Banfield and Eggleton 1990).

A number of studies imply crystallographic control on feldspar alteration. "Crystallographic control" as stated in this work includes line, plane and other defects inherent in original unaltered feldspar that may serve as preferential alteration sites, *and* crystallographic planes that are in direct contact with clay minerals. Parham (1969) presents evidence suggesting that line defects are favorable reaction sites. Berner and Holdren (1977) note that experimentally etched feldspar surfaces are pitted in oriented channels, suggesting that etching occurs where dislocations intersect the surfaces of feldspar grains. Eggleton and Buseck (1980) and other investigators describe holes in naturally altered feldspar bounded by (100), (101), (010) and (001), and note the association of alteration products with dislocations.

Feldspar microstructures that are susceptible to alteration may define passageways for aqueous fluids in feldspars; these can also be conduits for mass transfer of argon to and from the crystal interiors (Fitz Gerald 1993). The influence of crystallographic control on argon release kinetics in feldspars has been studied by Zeitler and Fitz Gerald (1986), Burgess et al. (1992), Fitz Gerald (1993), Parsons (1993) and Fitz Gerald and Harrison (1993). Incoherent or partially coherent grain boundaries between albite and microcline, both of which are regions of high defect density in perthites, are potential sites for argon migration into or out of feldspar (Burgess et al. 1992). Twin boundaries also

† Present address: Wittenberg University, Springfield, Ohio 45501.

https://doi.org/10.1346/CCMN.1997.0450310 Published online by Cambridge University Press

are proposed as sites for fast diffusion of argon (Zeitler and Fitz Gerald 1986).

Measured dissolution rates of minerals in a natural setting are typically slower by approximately 2 orders of magnitude than those measured in the laboratory (Swoboda-Colberg and Drever 1993). Experimental studies to determine feldspar dissolution rates indicate that feldspar dissolves congruently and that the reaction is surface-controlled, as opposed to volume-diffusion-controlled (Berner 1981; Sverdrup 1990). The reacting surface area of the parent mineral undergoing dissolution is not well known and may be overestimated in the laboratory (Rowe and Brantley 1993). Dissolution-rate constants are determined from experimental runs on different-size fractions of crushed feldspar grains. Crushed grains used as starting material for dissolution experiments are not necessarily subjected to the same physical conditions that exist in nature (Casey et al. 1993). For example, crushing in the laboratory may induce breakage along cleavage directions or fractures, but natural specimens may not undergo the same mechanical changes prior to dissolution.

Experimentally determined mineral dissolution rates are used in soil studies to model cation release rates during weathering. Models are important for judging the effect of weathering on the chemical properties of soils. Modeling the yield of cations such as K, Na, Ca and Mg that are released during weathering helps determine natural resistances to soil acidification (Sverdrup 1990). If chemical reactions producing clay minerals from parent feldspar are surface-controlled, potentially important surfaces for dissolution of natural specimens need to be determined to reconcile the discrepancy between field and laboratory dissolution rates.

In the present study, microcline perthite single crystals containing both altered and unaltered regions are observed with TEM, allowing direct determination of the spatial relationships between parent microtexture and clay alteration. "Altered regions" used here refers to feldspar microstructures immediately adjacent to or bounded by clay. The object of this work is to characterize altered regions to identify important surfaces involved in dissolution of feldspar and reprecipitation of clay minerals.

EXPERIMENTAL

Location and Geologic Setting

Microcline perthite crystals studied were collected from a weathered pegmatite in the Spruce Pine District, North Carolina. The geologic setting for this region is reported by Brobst (1962). Field and isotope studies conducted by Butler (1973) and a Rb/Sr isotope study of amphibolite country rocks surrounding Spruce Pine pegmatites (Goldberg et al. 1992) yield pegmatite emplacement ages of 390 Ma and 395 ± 6 Ma, respectively. Pegmatite emplacement is suggested to be approximately contemporaneous with regional metamorphism that occurred during the Acadian orogeny (Butler 1973).

Periods of uplift exposed Spruce Pine pegmatites, resulting in economically recoverable supergene kaolin deposits averaging 40 ft in thickness from the top of the parent rock but locally exceeding 100 ft (Parker 1949). Field evidence favoring a weathering origin for the kaolin deposits includes stream terraces containing old erosional surfaces capped by stratified sand and gravel deposits (Parker 1949).

Sampling and Methods

Microcline perthite single crystals were collected from a clay pit composed of altered pegmatite in the Gusher Knob/Brushy Creek district, located approximately 8 km northeast of Spruce Pine in Avery County, North Carolina. Three of the perthites were selected based on extent of alteration, from slightly altered to altered, as judged visually. These perthite crystals are brick-shaped with a maximum dimension of approximately 5 cm. Each perthite crystal contains altered and unaltered regions, allowing direct observation of the spatial relationships between parent microstructure and clay alteration.

Doubly polished petrographic thin sections of the crystals were made for examination by light-optical, electron microprobe (EMPA) and TEM methods. Sections were prepared parallel to (001) and (010); cleavage planes were used to orient the specimens. Highly altered perthites were impregnated with epoxy before preparing the thin sections.

Samples for TEM were extracted from the polished thin sections of oriented perthite. A Gatan ultrasonic disc cutter was used to drill standard 3-mm-diameter discs. The positions of the discs were selected at random. The main objective was to extract as many discs as possible from each thin section. Discs were supported with single-slot Cu grids and placed in a Gatan dual ion mill for final thinning by argon ion bombardment. Samples were lightly carbon-coated for examination by TEM.

Microtextural characterization was performed using a JEOL 200CX TEM in the Department of Materials Science and Engineering, The Ohio State University. The microscope was operated at an accelerating voltage of 200 kV. Qualitative chemical microanalyses were obtained in scanning TEM (STEM) mode using a Tracor Northern TN 2000 energy dispersive X-ray analyzer (EDS) fitted to the TEM. The volume of sample scanned during an analysis varied with the morphology and size of a region of interest and was controlled by changing the dimensions of the scan raster. All EDS analyses were counted for at least 100 s. Although the EDS data are qualitative, they provided the

Table 1. EMPA of microcline host and film albite lamellae.

Analysis	wt% oxide								mol% endmember			Phase
	SiO_2	Al_2O_3	MgO	CaO	FeO	Na_2O	K_2O	Total	Or	Ab	An	
1	64.75	18.92	0.00	0.03	0.07	3.35	13.00	100.12	71.60	28.12	0.12	host
2	63.87	18.69	0.00	0.01	0.00	1.27	15.31	99.16	88.73	11.17	0.10	host
3	64.18	18.53	0.00	0.00	0.02	0.69	16.31	99.73	94.00	6.00	0.00	host
4	68.34	19.87	0.00	0.32	0.09	11.01	0.13	99.76	0.73	97.69	1.58	lamella
5	64.96	18.52	0.02	0.00	0.06	0.99	15.88	100.43	91.31	8.69	0.00	host
6	64.54	18.65	0.01	0.00	0.02	0.50	16.37	100.09	95.53	4.47	0.00	host
7	68.26	19.90	0.01	0.18	0.15	11.12	0.06	99.66	0.380	98.76	0.86	lamella
8	68.03	19.88	0.01	0.36	0.06	11.03	0.12	99.50	0.70	97.54	1.77	lamella
9	68.48	19.96	0.00	0.40	0.14	11.09	0.08	100.14	0.44	97.63	1.94	lamella
10	67.93	19.78	0.00	0.21	0.07	11.19	0.06	99.24	0.32	98.64	1.03	lamella
11	68.38	19.76	0.04	0.21	0.16	11.18	0.08	99.80	0.44	98.53	1.03	lamella
12	68.36	19.87	0.00	0.27	0.10	11.43	0.06	100.09	0.36	98.35	1.29	lamella
13	67.27	20.16	0.00	0.40	0.00	11.07	0.08	98.98	0.94	97.52	1.53	lamella
14	64.64	18.60	0.00	0.01	0.10	1.05	15.81	100.12	90.84	9.12	0.04	host
15	64.55	18.49	0.00	0.03	0.00	0.57	16.85	100.49	94.99	4.85	0.16	host
16	67.14	19.89	0.03	0.27	0.06	11.09	0.09	98.57	0.52	98.15	1.33	lamella
17	64.31	18.42	0.01	0.02	0.00	0.71	16.28	99.74	93.69	6.22	0.09	host
18	64.21	18.75	0.00	0.00	0.04	0.67	16.76	100.42	94.25	5.75	0.00	host

means to discriminate between complex twin lamellae in K-rich and similar size Na-rich exsolution lamellae. Quantitative EMPA data were obtained to confirm that the small-scale perthitic lamellae seen in TEM were indeed albite.

EMPA was performed using a Cameca SX-50 electron microprobe in the Department of Geological Sciences, The Ohio State University. Analyses were made at 15 kV and 20 nA on a visually unaltered perthite specimen cut parallel to (010). The smallest albite lamellae analyzed were a few μm wide, limited by the approximately 1-μm electron probe spot size.

RESULTS

Light-Optical Microscopy

Light-optical study of specimens viewed subparallel to c* reveals cross-hatched twinned host microcline (K-rich) containing less abundant albite plagioclase lamellae (Na-rich); EMPA data obtained from these phases are presented in Table 1. This texture is characteristic of slowly cooled microcline perthites (see Fitz Gerald and McLaren, 1982, for pertinent references). Light-optical micrographs of a representative ion-thinned sample are shown in Figures 1a and 1b. The specimen is rotated so that (010) twin composition planes in albite appear as parallel bands in the upper left portion of Figure 1a. Albite-twin individuals such as these are wide and therefore easily distinguished from thin albite-twin individuals in microcline. Following Andersen's terminology (1928), vein and film albite are visible in transmitted light (Figure 1a). Vein albite lamellae approach 100 μm in maximum width and are mm-scale in length. Film albite lamellae approach 10 μm in width and are tens to hundreds of μm in length.

Grain boundaries between vein albite and cross-hatched microcline are irregular (Figure 1a). In contrast, film albite/microcline boundaries are regular with the long dimensions of film albite approximately parallel to the *b*-axis of microcline. Film albite/microcline boundaries do not appear to change in crystallographic orientation compared to vein albite/microcline boundaries (Figure 1a). Generally, film albite is concentrated in turbid regions between large vein albite lamellae.

Perthite, positioned in Figure 1b so that albite-twin lamellae are in the extinction position, shows the alteration most clearly. Feldspar altered to clay appears as medium gray, irregular stringers that cross-cut the sample, and is concentrated in the following areas: within vein albite grains, at the grain-boundary margins between vein albite and microcline and at microcline/film albite boundaries. The clay within vein albite is easily recognized; this aided identification of alteration channels in microcline. The specimen may have fractured along alteration channels during sample preparation: however, the channels appear to contain clay, which suggests that they are not an artifact of sample preparation.

TEM of Unaltered Regions

The term "unaltered" herein applies to regions in perthite that do not contain clay. Nonetheless, these regions may have undergone substantial changes since the time of crystallization. Some of the described features may be associated with processes leading to clay formation.

VEIN ALBITE. Vein albite lamellae are recognized in TEM images by the large widths of their albite twins, as observed in transmitted light (Figure 1a). Although boundaries between vein albite and microcline are ir-

https://doi.org/10.1346/CCMN.1997.0450310 Published online by Cambridge University Press

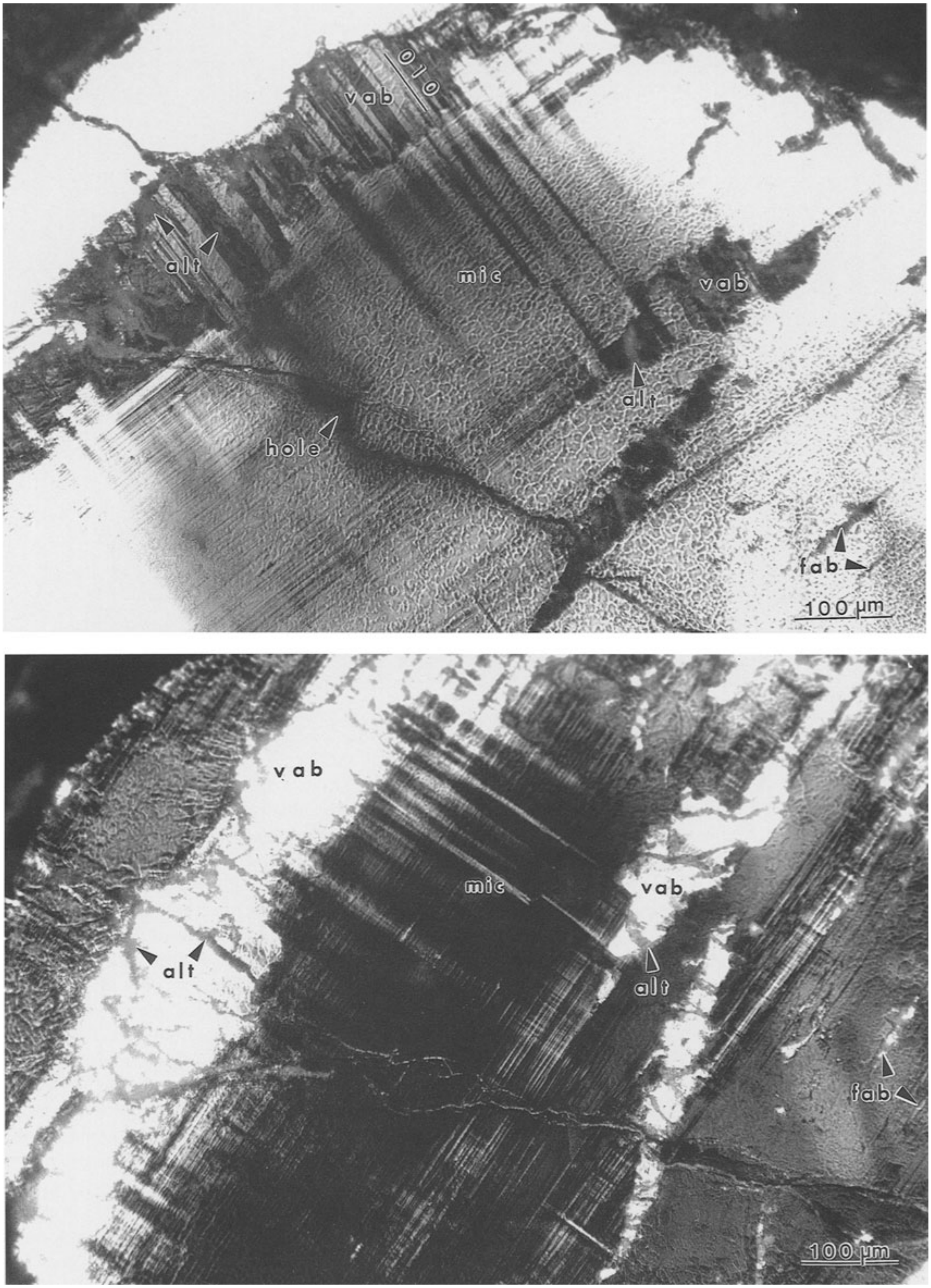

Figure 1. a) Light-optical micrograph of an ion-thinned specimen rotated to the parallel position, that is, (010) twin individuals are evident in vein albite ("vab"). Film albite ("fab"), cross-hatched twinned microcline ("mic"), alteration ("alt") and a hole produced by ion milling are also indicated. b) Same region shown in Figure 1a rotated so that (010) twin individuals in vein albite are extinguished. Light gray stringers of clay ("alt") cut across vein albite ("vab") and film albite ("fab").

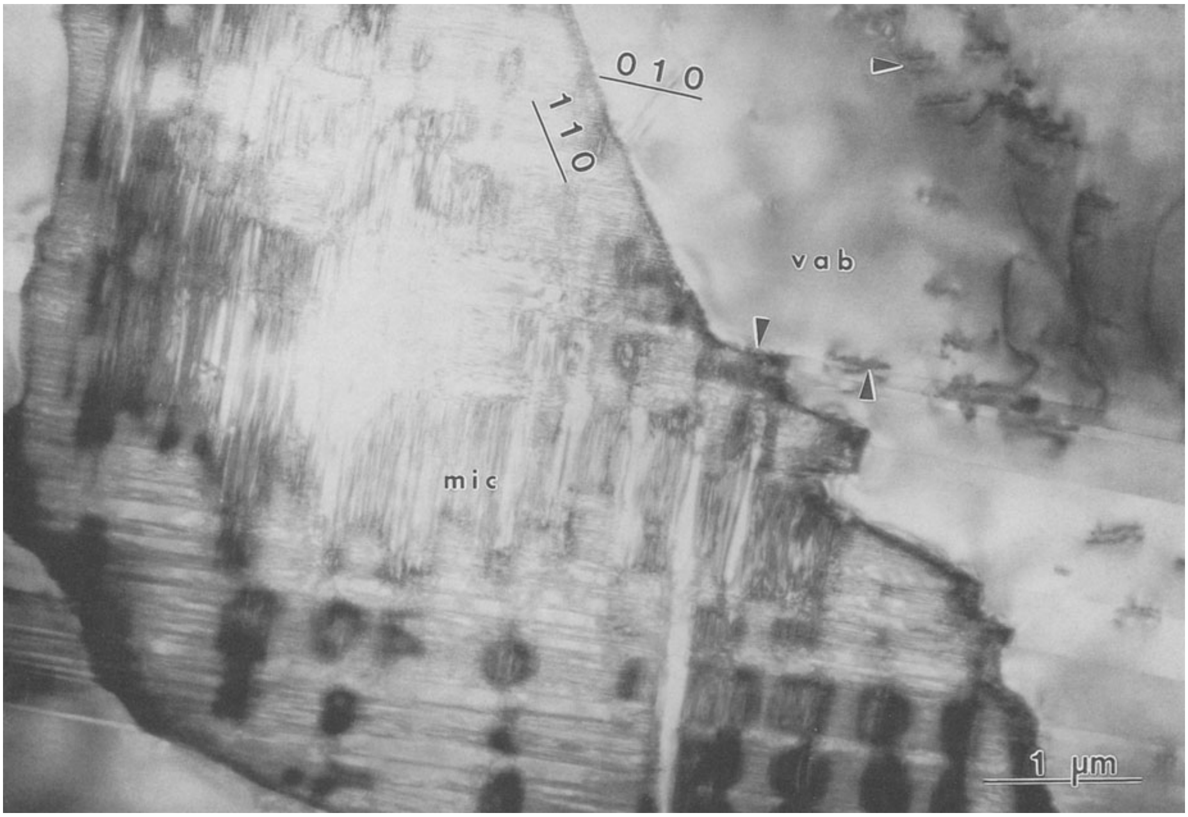

Figure 2. [102] BF image of microcline ("mic")/vein albite ("vab") grain boundaries. Boundary traces parallel (010) and {110} of microcline. Dislocations (arrowed) are located adjacent to and within the grain boundaries.

regular when viewed in transmitted light, planar interfaces predominate when viewed with TEM.

A common planar boundary is (010), easily recognized because its trace parallels the trace of albite twin composition planes. Another common planar boundary makes an angle of approximately 35° with respect to b* of microcline. This plane corresponds to (110) or ($1\bar{1}0$) in microcline. These traces are hereafter referred to as the *hkl* form {110}. A [102] bright field (BF) image showing the (010) and {110} grain-boundary orientations between vein albite and microcline is shown in Figure 2. Dislocations are common in vein albite, and occasionally are aligned parallel to the orientation of the albite/microcline grain boundaries. Dislocations also are observed in contact with grain boundaries.

FILM ALBITE LAMELLAE. No images were obtained of unaltered film albite.

CRYPTOPERTHITIC ALBITE LAMELLAE. Cryptoperthite is either untwinned or contains regions of very small-scale albite twinning (0.01 to 0.1 μm). These albite lamellae are lens-shaped and average a few tenths of a μm in width (Figure 3). The lengths of the albite lamellae parallel the *b*-axis of microcline and, thus, the lamellae have (*h0l*)-type habit planes with microcline. (The precise orientation relationship between these lamellae and the host phase was not determined because this requires observations from samples viewed nearly parallel to [010] of the host, and all TEM observations herein were nearly parallel to c*.) Regions in microcline containing fine-scale albite twins (Figure 3, right) alternate with long strips of untwinned microcline (Figure 3, left). Occasionally, albite lamellae extend over the boundary between small-scale albite twinned and untwinned microcline. When this occurs the Na-rich lamellae may be untwinned with respect to the albite law. This suggests that twinning in microcline may be initiated by strain from substantial numbers of Na-rich lamellae, as proposed by Tibballs and Olsen (1977).

Distinguishing pericline twin lamellae in the microcline host from cryptoperthitic albite exsolution lamellae is accomplished by imaging in near 2-beam conditions (McLaren 1978). Both types of lamellae are similar in size and elongate parallel to [010] of microcline. However, when a specimen is tilted so that only the ($20\bar{1}$) reflection is diffracting strongly, pericline twin lamellae extinguish and albite lamellae are visible. In practice, if the reciprocal lattice row containing

https://doi.org/10.1346/CCMN.1997.0450310 Published online by Cambridge University Press

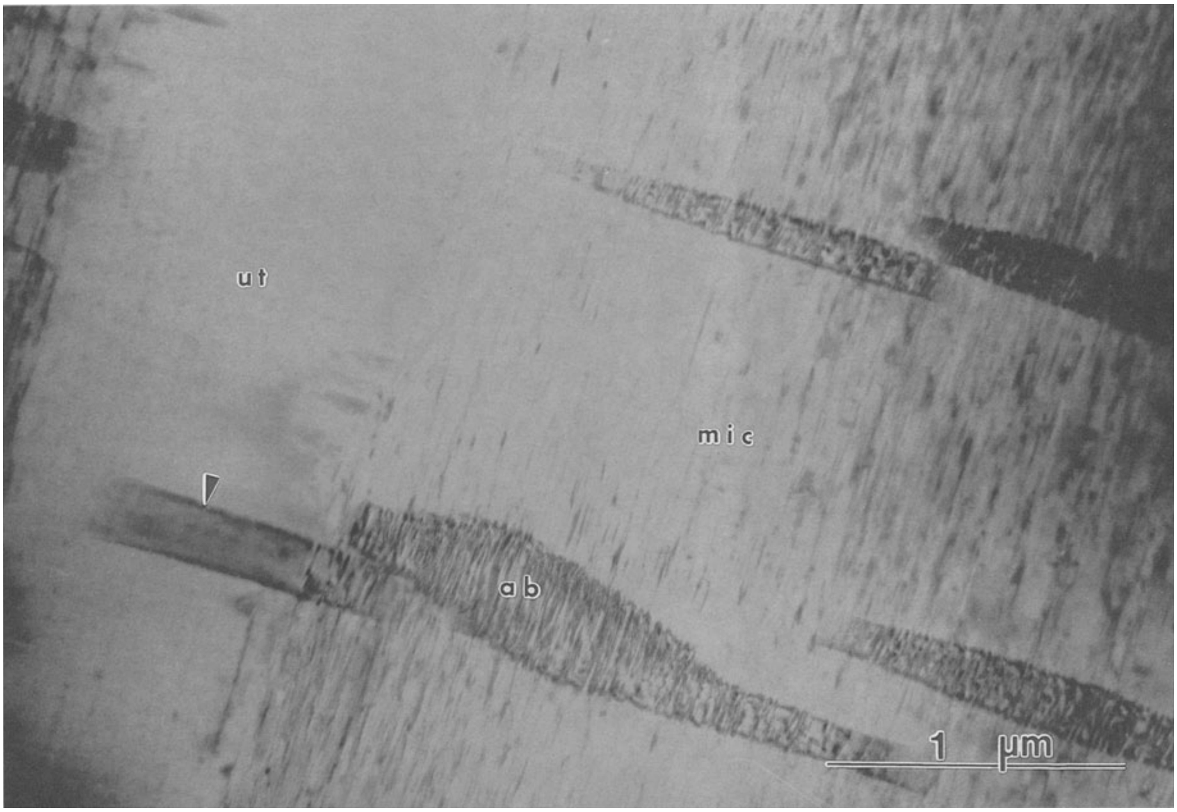

Figure 3. [102] BF image of small-scale albite-twinned cryptoperthitic texture. Albite-twinned microcline ("mic") contains lens-shaped albite exsolution lamellae ("ab") of submicron scale thickness. An exsolution lamella (arrowed) is untwinned where it overlaps untwinned ("ut") microcline.

$(20\bar{1})$ is strongly diffracting, the pericline twins are extinguished. Pericline lamellae in microcline imaged under these conditions are out of contrast and appear gray, whereas cryptoperthitic albite exsolution lamellae appear white (Figure 4).

TWINNING IN HOST MICROCLINE. Spruce Pine perthites contain albite- and pericline-twinned microcline, similar to twinning textures observed in other slowly cooled alkali feldspars (Akizuki 1972; Tibballs and Olsen 1977; McLaren 1978; Fitz Gerald and McLaren 1982). TEM reveals domains that contain albite and pericline twins whose individual lamellar widths range from hundredths of μm to tens of μm. Twin domains occasionally are interrupted by untwinned regions that vary in size. The use of the term "untwinned" in describing a microcline perthite is always a question of scale.

Some regions of microcline consist of alternating albite-twinned and untwinned lamellae (Figure 5) whose long dimensions approximately parallel [010]. This twinning texture also is reported by Akizuki (1972) in a Spruce Pine specimen. The width of the albite-twinned lamellae ranges from approximately 0.1 to 1 μm. Albite twins occasionally extend into neighboring untwinned zones or pericline twin lamellae (Figure 5); the latter suggests that pericline-twinned domains apparently are converting to albite twins. Some untwinned zones contain narrow bands of wavy contrast, oriented approximately parallel to [010] (Figure 5). The ends of the albite-twin lamellae in some places terminate at the narrow bands (Figure 5).

A twinning texture observed in the K-rich microcline that is not discussed in detail in the literature consists of coarsely albite-twinned regions "decorated" with small (0.01–0.1 μm wide) lens-shaped "nuclei" (Figure 4, lower right). The long axes of these small-scale exsolution lamellae are perpendicular to the trace of the (010) albite-twin boundaries. The nuclei share the same contrast (and therefore orientation) as the elongate albite lamellae identified using EDS. Some nuclei appear in clusters trending parallel to the trace of (010), but in regions where no albite twin boundaries are visible, suggesting a homogeneous nucleation mechanism of formation.

HOLES AND MICROFRACTURES. Holes observed average a few tenths of a μm in cross section; their boundaries often represent principal crystallographic directions as projected on the image plane. These traces include

https://doi.org/10.1346/CCMN.1997.0450310 Published online by Cambridge University Press

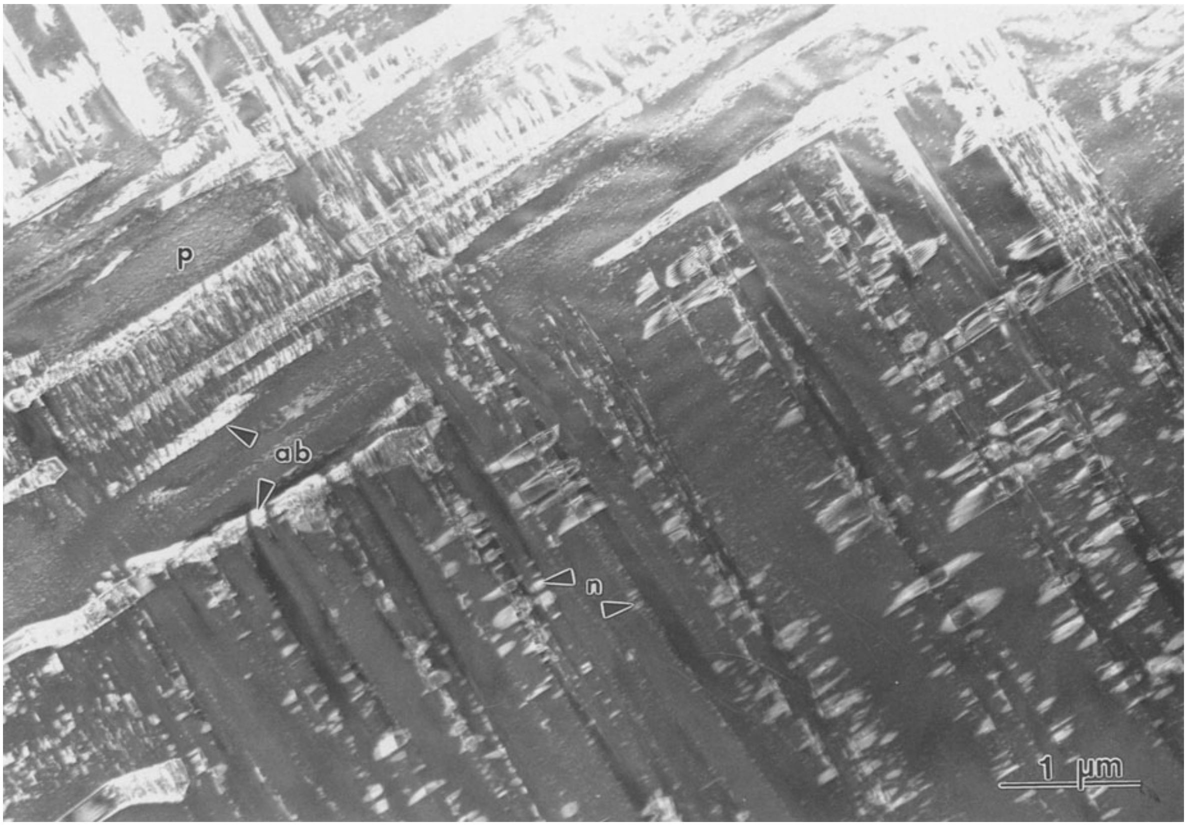

Figure 4. Two-beam DF image recorded with ($20\bar{1}$) as the operating reflection. Cryptoperthitic albite exsolution lamellae ("ab") and nuclei ("n") both appear white in this orientation. Pericline-twin composition planes ("p") are extinguished in this orientation.

(010), {110}, and {*h0l*} of microcline; the latter represent the traces of planes approximately parallel to pericline-twin composition planes, and are associated with large-scale albite/microcline grain boundaries, misoriented twin domains, microfractures, dislocations and regions containing alteration to clay. Some holes have irregular boundaries and may represent original microstructure; however, they are not confirmed as such because of confusion with damage resulting from ion-milling.

Some holes having linear boundaries are associated with microfractures in host microcline. A [102] BF image of such a fracture is presented in Figure 6. This microfracture trends approximately parallel to the trace of {110} planes in microcline. Holes with boundaries parallel to (010) and {110} of microcline are observed within the microfracture. The fracture cuts across albite and pericline twinning domains. Fractures occasionally are observed to grade into bands of dislocations aligned subparallel to {110}. Other orientations are present also.

TEM of Altered Regions in Spruce Pine Perthites

CHARACTERIZATION OF CLAY MINERAL ALTERATION. Halloysite is recognized in TEM by its characteristic rolled, layer morphology (Figure 7). Halloysite is present in void spaces detached from feldspar and also forms grain-boundary interfaces with microcline and vein or film albite. The fact that halloysite often is detached is most likely an artifact of sample preparation. Halloysite is prone to thin much more rapidly than feldspar with argon ion bombardment. Therefore, mineral phase boundaries that include halloysite in adequately thin regions are comparatively rare.

The rolled morphology halloysite exhibits may represent either spheres or tubes viewed lengthwise. Halloysite is occasionally polygonal in outline and shows well-developed contrast lines that separate layers (Figure 7). These layer separations may result from electron-beam dehydration (Kohyama et al. 1978), from dehydration during sample preparation before examination by TEM (Gard 1972) or from dehydration in nature. Identification of halloysite is supported by qualitative EDS, powder XRD and selected area diffraction (SAD). The latter produces ring patterns whose *d*-values match those of halloysite, the largest of which is 7 Å (Figure 7, inset, arrowed). Intensities and *d*-values are similar to those given in Brindley (1951).

ALTERATION OF ALBITE. Halloysite is often detached from large-scale albite lamellae in thin, electron-transparent

https://doi.org/10.1346/CCMN.1997.0450310 Published online by Cambridge University Press

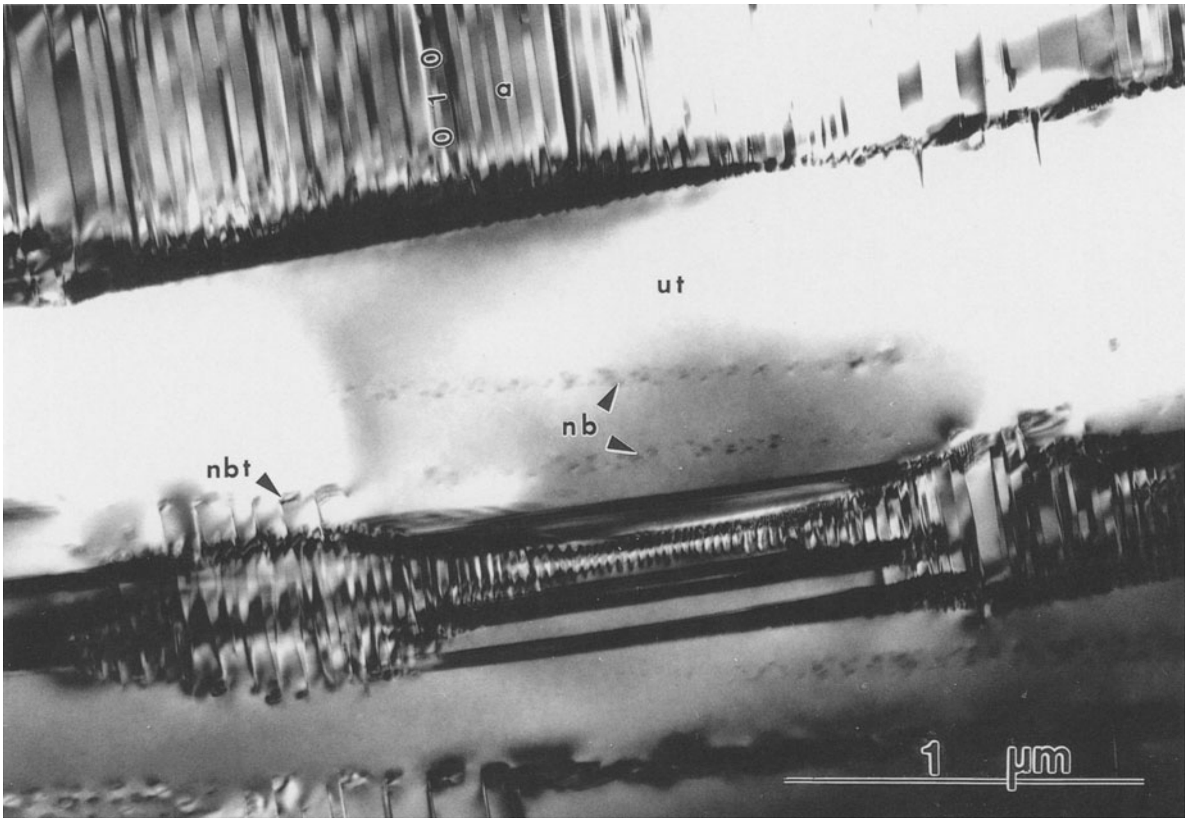

Figure 5. BF image of a twinning domain in microcline containing narrow bands of contrast ("nb") that occasionally inhibit the extension of albite twins into untwinned regions ("nbt"). Albite-twinning ("a") and an untwinned region ("ut") also are indicated.

regions, and it is difficult to determine if the halloysite has moved during ion milling (Figure 8). Albite/halloysite contacts generally are nonlinear and irregular. These are sites of the most areally extensive alteration to halloysite. In contrast, cryptoperthitic albite lamellae are not replaced by halloysite within microcline.

ALTERATION OF MICROCLINE. Planar contacts between microcline and halloysite are observed more frequently than are planar albite/halloysite contacts. Halloysite exists in cavities and channels in microcline. Some of these clay/feldspar interfaces parallel the traces of (010) and {110} of microcline, similar to the planar contacts that form holes and microfractures. Other planar boundaries are also observed but have not been indexed. Some alteration interfaces contain micropores that extend into the microcline; these holes are bounded by planar traces, including (010) of microcline. Halloysite channels cut across all twinning textures observed in microcline.

An elongate channel of halloysite bounded on both sides by (010) of microcline is shown in Figure 9. The twinning texture of microcline in this region includes an untwinned zone and a pericline-twinned zone bounding the halloysite channel. Faint contrast lines parallel to (010) in the pericline-twinned zone may represent pericline twins partially converted to albite twins or albite-twinned albite exsolution lamellae. Halloysite rolls are well developed adjacent to the pericline twinning. The boundary between halloysite and pericline-twinned microcline is less regular, but close inspection reveals that this boundary is composed of small-scale planar contacts parallel to (010) of microcline.

Halloysite channels also are observed in the vicinity of microfractured microcline. An example of such a fracture, whose trace trends subparallel to {110} of microcline, is shown in Figures 10a and 10b. A hole located on the fracture trace has boundaries parallel to (010) and {110} of microcline (Figure 10a). A 1–2-μm-wide halloysite channel bounded by {110} of microcline is observed within several μm of this microfracture in the same TEM specimen and along the same trace (Figure 10b).

DISCUSSION

Microtextural elements in Spruce Pine perthites are discussed herein as potential preferred sites for dissolution/reprecipitation during alteration. A brief consideration of possible reaction mechanisms follows.

Figure 6. BF image of microfracture in microcline cutting albite ("a") and pericline ("p") twinning. Albite twin planes are displaced across the fracture as along a fault. The fracture trace parallels {110}. Holes are developed along the fracture with boundary traces parallel to (010) and {110}.

Albite/Microcline Phase Boundaries

Phase boundaries in perthites may be mostly coherent, as shown by high-resolution TEM (HRTEM) of cryptoperthites (Brown and Parsons 1984b). Criteria used to define a coherent boundary include minimal disruption of crystal structure when crossing the phase boundary and a subsequent lack of dislocations in the boundary (Parsons and Brown 1984). Because of the regularity in crystallographic orientation of grain boundaries between microcline and cryptoperthitic albite, such boundaries are thought to be less susceptible to alteration than are large-scale albite/microcline boundaries. In this study dislocations are not observed on cryptoperthite/microcline boundaries (Figure 3). In addition, cryptoperthitic lamellae are not observed to be replaced preferentially by halloysite. Parsons (1993) suggests that cryptoperthite is a coherent texture that is not conducive to fluid transport.

On the contrary, coarsened lamellar phases in perthites, such as vein albite (Figures 1 and 2), and film albite (not shown) have incoherent boundaries with the host phase (Smith and Brown 1988). Worden et al. (1990) observe, in perthites from the Klokken syenite, the progression from perthite with coherent lamellar boundaries to deuterically coarsened perthite with incoherent lamellar boundaries over a sharp contact only a few μm across. These authors observe both a notable increase in the population of holes and a change in albite grain boundary orientation from ($\bar{6}\bar{6}1$) to (010) of the microcline in association with the change to deuterically coarsened perthite texture. Secondary mineralization including clays and Fe-oxides is also observed in the deuterically altered regions (Worden et al. 1990).

Dislocations are always observed adjacent to vein albite/microcline boundaries and sometimes directly on these boundaries. The projection of images of dislocation lines on the plane of the specimen shows that they are aligned parallel to the trace of (010) twin planes in vein albite (Figure 2). Dislocations in (010) may be important conduits for fluids during the formation of vein albite. These dislocations also may be important for halloysite formation where vein albite and microcline are adjacent. The boundaries are among the most strongly altered zones in the Spruce Pine perthites (as seen in transmitted light and TEM).

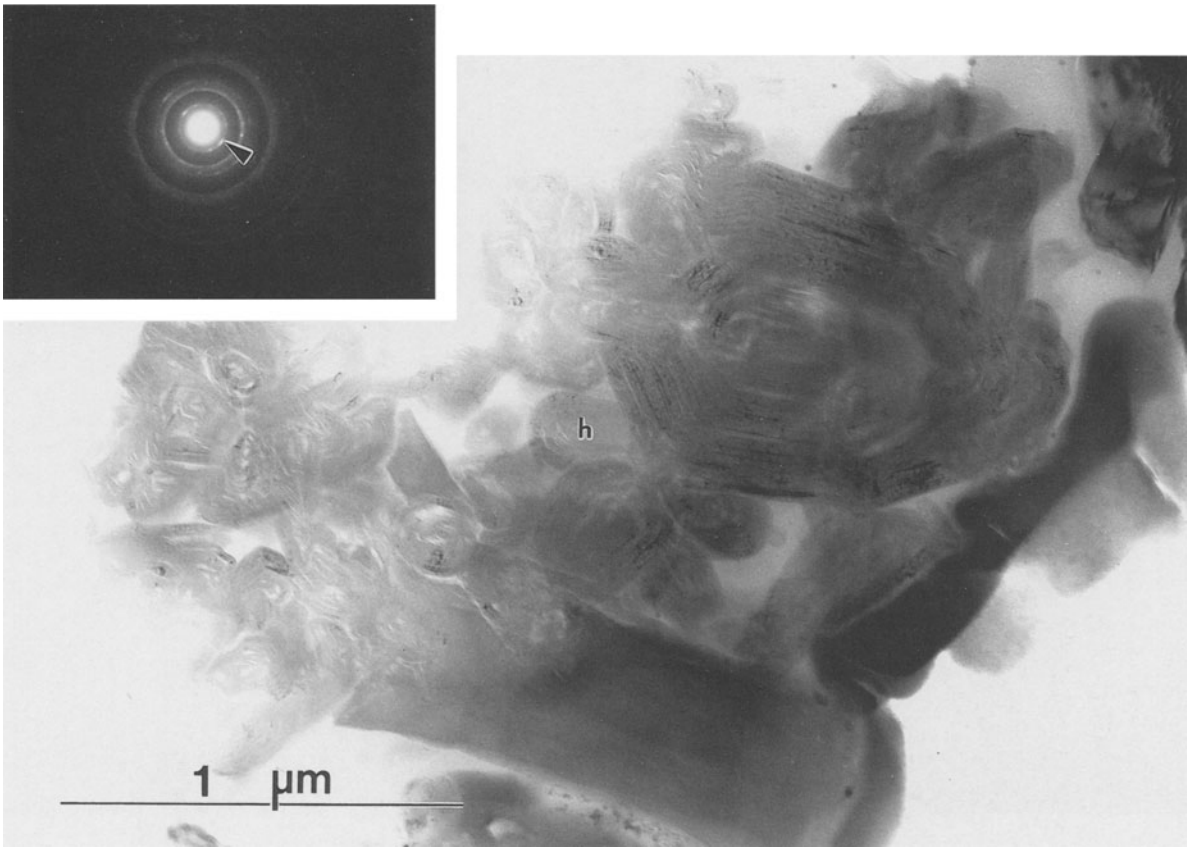

Figure 7. BF image of halloysite ("h") showing rolled layer morphology. Inset electron diffraction pattern contains *d*-spacings consistent with dehydrated halloysite; 7-Å *d*-value is arrowed.

Twin Composition Planes

Although little structural mismatch exists between twin individuals along (010) for albite twins and along the rhombic section for pericline twins, Smith and Brown (1988) suggest that dislocations must accommodate the structural recrystallization that occurs when the orientation of the rhombic section (pericline twin composition plane) changes with cooling. Because dislocations may serve as conduits for fluids, it is possible that twin composition planes may act as preferred sites for alteration.

SAD analysis of Spruce Pine twin textures indicates that the albite-twin orientation is dominant in microcline, in accord with Akizuki (1972), Tibballs and Olsen (1977) and Fitz Gerald and McLaren (1982). Apparent conversion of pericline twins to albite twins, that is, extension of the latter into regions of the former (Figure 5), suggests that the stability of albite twinning relative to pericline twinning increases with cooling (Fitz Gerald and McLaren 1982). Fitz Gerald and McLaren also indicate that strained regions in the crystal occur where albite twins intersect pericline twins in microcline. Electron-beam damage is observed to occur preferentially in these twin overlap regions in the present study.

No distinction is made between the relative susceptibility to alteration of pericline and albite twins with the present TEM data. Unaltered, twinned regions that include all of the observed twin domains in microcline are cross-cut by approximately 1-µm-wide channels of halloysite. However, in some regions of microcline, alteration to halloysite extends preferentially into twinned zones as opposed to untwinned zones (Figure 9), suggesting that once alteration to clay begins, dissolution and replacement of microcline by clay occurs more readily in strongly twinned zones.

Nuclei

Nuclei that are observed along albite twin composition planes in microcline (Figure 4) are interpreted as small-scale albite exsolution lamellae, but their small grain size inhibits chemical identification by EDS. EDS of nuclei does not produce a Na peak to verify their identity. Moreover, small cryptoperthite lamellae, but larger than nuclei, do not produce a Na peak significantly above background. This possibly is

https://doi.org/10.1346/CCMN.1997.0450310 Published online by Cambridge University Press

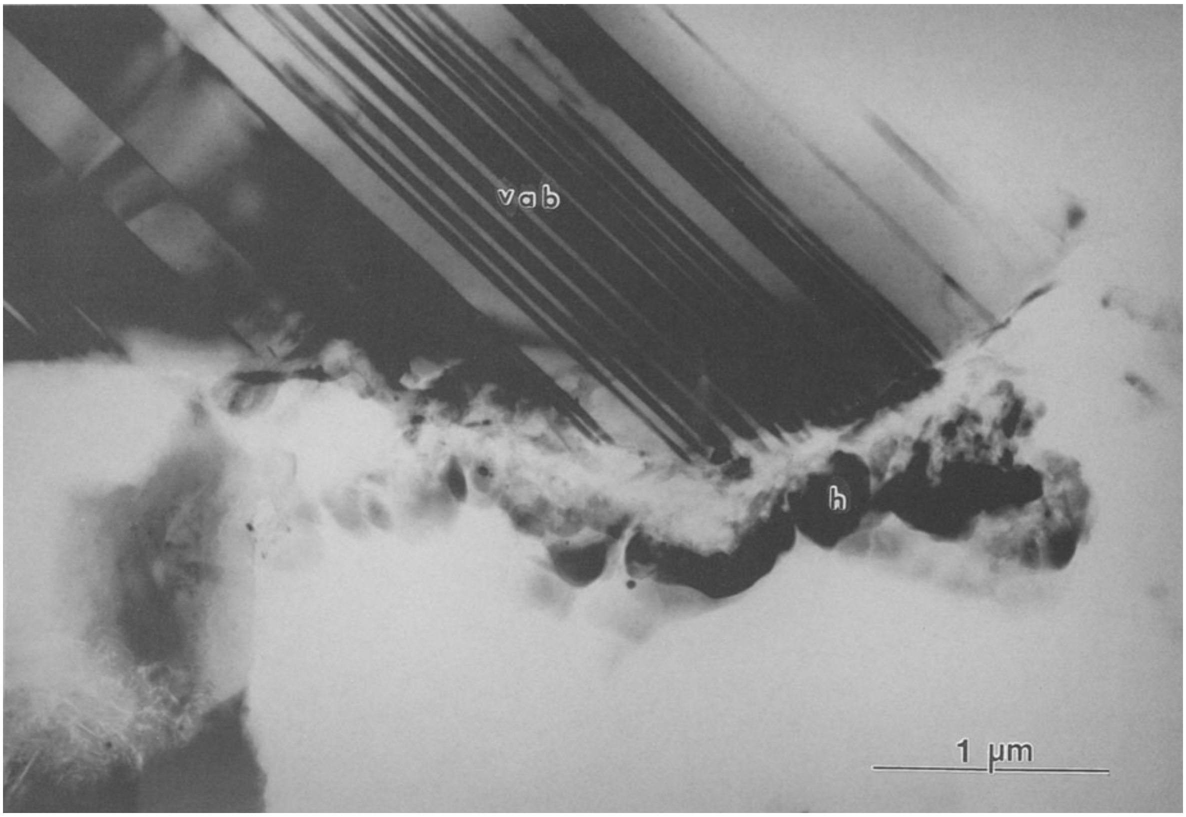

Figure 8. BF image containing a vein albite ("vab")/halloysite ("h") grain boundary. Halloysite shown in this photo may have moved during specimen preparation.

due to the orientation of the lamellae with respect to the cut surfaces of the TEM samples, which are approximately parallel to (001) of K-feldspar. The albite lamellae have (*h0l*) habit planes and therefore are inclined to the electron beam.

Smith and Brown (1988) discuss a texture in an antiperthite that is similar to regions containing "nuclei" described here. They attribute the formation of this small-scale antiperthitic texture to both homogeneous and heterogeneous nucleation; the latter is accomplished by preferential nucleation at pre-existing twin planes.

Narrow bands oriented approximately parallel to [010] in untwinned microcline (Figure 5) show contrast that is similar to the "nuclei" and Na-rich cryptoperthitic exsolution lamellae (Figure 4). Brown and Parsons (1983) observe similar features that they term "speckled contrast", and attribute the features to Na-rich exsolution "platelets" that homogeneously nucleate in a K-rich host. The similar contrast exhibited by the nuclei *and* the narrow bands to the cryptoperthite suggests that the former are possibly late-stage exsolution lamellae in the Spruce Pine perthites.

Similar to cryptoperthitic albite lamellae, the narrow bands of contrast and "nuclei" are not observed to be replaced preferentially by clay. Therefore, these microtextural elements are not considered to be important sites for the development of alteration in Spruce Pine perthites.

Holes

Holes are a common feature of feldspars, and a number of terms to describe them appear in the literature. For instance, Eggleton and Buseck (1980) term them "negative crystals" and "vacuoles" in a TEM study of weathered feldspar. Burgess et al. (1992) term holes observed in deuterically altered perthites as "micropores". We use the term "holes" to describe any void space in the interior of the perthites regardless of the degree of regularity of their boundaries.

Holes in Spruce Pine perthites that have determinable crystallographic boundaries are interpreted to have been present in the perthites prior to sample preparation. Holes with linear boundaries, as shown in (001) TEM sections, include those bounded by the traces of {110} and (010) of microcline (Figure 6). Other orientations are present that have not been "indexed" (not illustrated). Holes also may be produced by ion milling, but these are bounded by nonplanar

https://doi.org/10.1346/CCMN.1997.0450310 Published online by Cambridge University Press

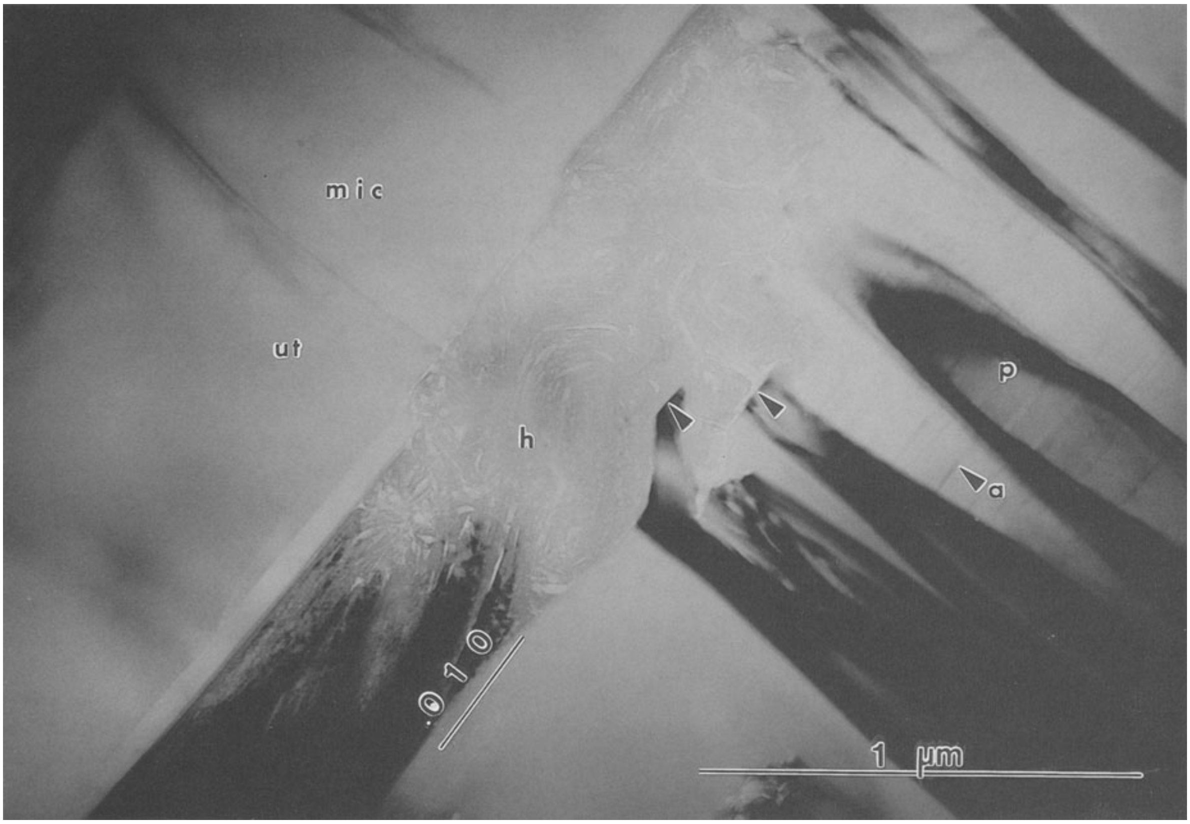

Figure 9. BF image of an elongate channel of halloysite ("h") in microcline ("mic"). Microcline/halloysite boundaries parallel (010) and abut untwinned areas ("ut") in microcline. This halloysite channel widens in the vicinity of pericline twinning ("p"). Faint contrast lines ("a") represent either pericline twins partially converted to albite twins or albite-twinned albite exsolution lamellae. Halloysite/pericline-twinned microcline boundary contains planar (010) contacts (arrows).

outlines that bear no geometric relation to the microtexture of the sample.

Hole boundaries in the Spruce Pine specimens are similar to those found in the Klokken syenite. Klokken perthites include traces of holes (in 001 sections) that are commonly irregular, but some are bounded by (010) and {110}; this is observed both in ion-milled TEM and (001)-cleaved SEM images, so hole geometry is not considered to be an artifact of the ion-thinning process (Worden et al. 1990).

The similarity in hole geometry of Spruce Pine specimens with that of the Klokken perthite is noteworthy because the Klokken is quite different chemically, with an "intermediate" bulk composition of $Or_{32}Ab_{67}An_1$ (Brown and Parsons 1984b). Bulk chemical data for the Spruce Pine microcline perthites of the present study were not obtained. However, bulk analyses of the microcline perthite sample from Spruce Pine studied by Akizuki (1972) yield a composition of $Or_{78}Ab_{22}An_0$. This suggests that the orientations and geometries of micropores in alkali feldspars do not change as a function of chemical composition, even though microtextures accompanying these different compositions are variable.

Holes in Spruce Pine perthites are not observed in association with cryptoperthitic lamellae. This agrees with Klokken perthites (Worden et al. 1990); these authors show that holes occur only in areas where lamellae are coarse and twinning in K-feldspar is extensive. David and Walker (1990) observe that ^{18}O, used as a tracer isotope for samples reacted with 99% $H_2{}^{18}O$ at 700 °C, preferentially penetrates into "turbid", coarse regions that contain more holes, as opposed to areas with small lamellae that do not contain holes. This demonstrates that regions containing large lamellae are more permeable to solutions (David and Walker 1990). In addition, although holes imaged in feldspars are attributed to formation during weathering (Eggleton and Buseck 1980), Klokken perthite micropores are suggested to be formed during deuteric coarsening prior to weathering (David and Walker 1990).

Slip Systems and Microfractures

The planes (010) and {110} are prominent cleavage and parting directions in alkali feldspar (Smith and Brown 1988) and also define slip systems and fracture planes. Slip in feldspars generally is achieved only at high temperatures experimentally but may occur in na-

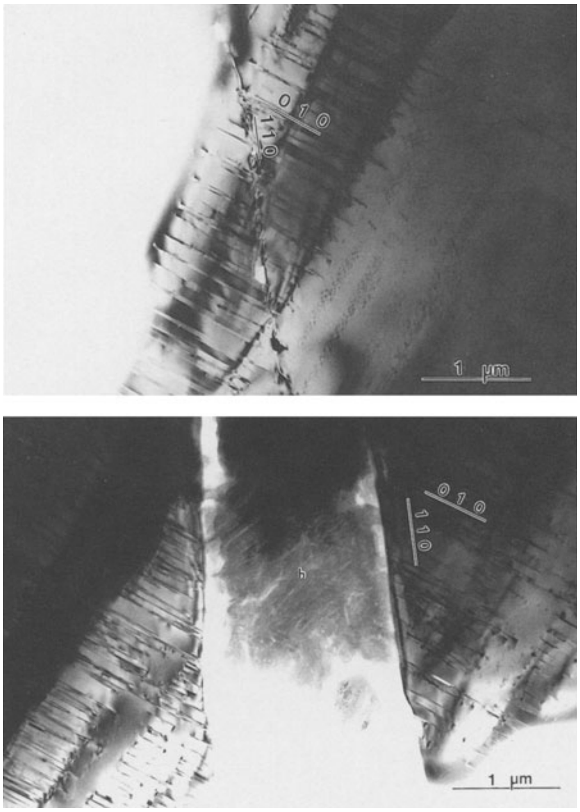

Figure 10. a) [102] BF image of a microfracture in microcline trending subparallel to the trace of {110}. The fracture can be traced to a channel infilled with halloysite (next figure). b) [102] BF image of microcline altered to halloysite ("h"); this image was recorded from the same sample and near the same region shown in Figure 10a. Microcline/halloysite boundaries are subparallel to {110}.

ture at low temperatures and strain rates over geologic time (Gandais and Williame 1984). Water also may encourage ductile behavior at low temperatures (Gandais and Williame 1984). Analyses of defects in experimentally deformed sanidine using TEM indicate that the most prominent slip systems are (010)[001], (010)[101] and (121)[101] at low experimental temperatures (T = 700 °C). The less important system (110)1/2[112] is also observed along with others (Gandais and Williame 1984).

A light-optical study of naturally deformed microcline perthite crystals from Arize, France, shows that the prominent slip planes are (001) and {110} at an estimated temperature of 550 °C (Debat et al. 1978). Tension gashes infilled with sigmoidally shaped albite lamellae are bounded by {110} slip planes. These authors hypothesize that (010) could be a key glide plane for deformation. Debat et al. (1978) note an increase in the amount of perthite for more strongly deformed specimens and postulate that perthite formation has a mechanical origin in this case. A light-optical study of microfracturing of plagioclase in a meta-anorthosite, which was naturally deformed under brittle conditions, shows that (001), (010), (110) and ($1\bar{1}0$) are important fracture planes (Brown and Macaudiere 1984).

The present observations on (001) sections of Spruce Pine perthites suggest that (010) and {110} planes impart control for fluid-induced changes of the crystal structure: (010) are prominent cleavage directions and {110} are prominent parting directions, especially in perthites (Smith and Brown 1988). Halloysite-infilled channels along {110} (Figure 10b) and planar contacts between halloysite and (010) of microcline (Figure 9) suggest that these are important surfaces in chemical reactions involving replacement of microcline by clay.

Reaction Mechanisms

Berner (1981) discusses possible mechanisms for dissolution and replacement of minerals during alteration reactions. These include surface-controlled, transport-controlled and a combination of these 2 mechanisms. According to Berner (1981), a surface-controlled reaction produces dissolution pits in the parent mineral that are bounded by planar interfaces, which implies crystallographic control by the parent mineral. A surface reaction is thought to proceed preferentially at high-energy sites, such as at the "outcrops" of dislocations along the fluid/crystal interface (Berner 1981). A transport-controlled mechanism, on the other hand, produces irregular dissolution surfaces on the reacting parent crystal, implying the loss of crystallographic control on the alteration process (Berner 1981). Spruce Pine perthites show planar clay/feldspar boundaries, which indicates that the reaction is at least in part surface-controlled, and that important surfaces include (010) and {110}. The most extensively altered specimens contain negative crystals bounded by (010) and {110}, as well as others.

Holes with irregular boundaries are also noted, which indicates that the nature of the reaction may change to transport-controlled as alteration becomes more extensive. Nonplanar reaction boundaries between microcline and halloysite and between vein albite and halloysite suggest that crystallographic control is minimized after a certain point is reached in the reaction to clays, as suggested by Banfield and Eggleton (1990).

CONCLUSIONS

Crystallographic control of the alteration of microcline perthites from Spruce Pine is suggested by both light-optical and TEM data. The most important avenues for the passage of fluids are grain boundaries formed between vein and film albite with microcline, microfractures and holes. Moreover, halloysite channels cut across microcline to interconnect vein albite lamellae; this suggests that fluids that serve to coarsen film and vein albite lamellae may also initiate formation of halloysite. Vein albite/microcline grain boundaries, microfractures and hole boundaries follow (010) and {110}, which suggests that these are very important surfaces in the reaction of feldspars to clay. Strongly twinned regions appear to be favored over untwinned regions once the crystal has become permeable.

ACKNOWLEDGMENTS

This work was supported by grants from the Clay Minerals Society, the McCaughey Mineralogical Fellowship and a Graduate Student Alumni Research Award at the Ohio State University. J. M. Sheets acknowledges D. Little and H. Colijn for instruction and guidance at the Electron Microprobe and Electron Optics facilities at the Ohio State University. We appreciate the thoughtful reviews of R. A. Eggleton, K. A. Foland and J. Walker.

REFERENCES

Andersen O. 1928. The genesis of some types of feldspar from granite pegmatites. Nor Geol Tidsskr 10:116–207.

Akizuki M. 1972. Electron-microscopic investigation of microcline twinning. Am Mineral 57:797–808.

Banfield JF, Eggleton RA. 1990. Analytical transmission electron microscope studies of plagioclase, muscovite, and K-feldspar weathering. Clays Clay Miner 38:77–89.

Berner RA. 1981. Kinetics of weathering and diagenesis, Chapter 3. In: Ribbe PH, editor. Kinetics of geochemical processes. Rev Mineral vol. 8. Blacksburg, VA: Mineral Soc Am. p 111–133.

Berner RA, Holdren GR, Jr. 1977. Mechanism of feldspar weathering: I. Some observational evidence. Geology 5: 369–372.

Brindley GW. 1951. The kaolin minerals. In: Brindley GW, editor. X-ray identification and crystal structures of clay minerals. London: Mineral Soc. p 32–75.

Brobst DA. 1962. Geology of the Spruce Pine district, Avery, Mitchell, and Yancey counties, North Carolina. US Geol Surv Bull 1122A. 26 p.

Brown WL, Macaudiere J. 1984. Microfracturing in relation to atomic structure of plagioclase from a deformed meta-anorthosite. J Struct Geol 6:579–586.

Brown WL, Parsons, I. 1983. Nucleation on perthite-perthite boundaries and exsolution mechanisms in alkali feldspars. Phys Chem Mineral 10:55–61.

Brown WL, Parsons I. 1984b. Exsolution and coarsening mechanisms and kinetics in an ordered cryptoperthite series. Contrib Mineral Petrol 86:3–18.

Burgess R, Kelley SP, Parsons I, Walker FDL, Worden RH. 1992. ^{40}Ar-^{39}Ar analysis of perthite microtextures and fluid inclusions in alkali feldspars from the Klokken syenite, South Greenland. Earth Planet Sci Lett 109:147–167.

Butler JR. 1973. Paleozoic deformation and metamorphism in the Blue Ridge Thrust Sheet near Spruce Pine, North Carolina [abstract]. Geol Soc Am Abstr with Prog 5:382.

Casey WH, Banfield JF, Westrich HR, McLaughlin L. 1993. What do dissolution experiments tell us about natural weathering? Chem Geol 105:1–15.

David F, Walker L. 1990. Ion microprobe study of intragrain micropermeability in alkali feldspars. Contrib Mineral Petrol 106:124–128.

Debat P, Soula J-C, Kubin L, Vidal J-L. 1978. Optical studies of natural deformation microstructures in feldspars (gneiss and pegmatites from Occitania, southern France). Lithos 11:133–145.

Eggleton RA. 1986. The relation between crystal structure and silicate weathering rates. In: S. M. Coleman and D. P. Dethier, editors. Rates of chemical weathering of rocks and minerals. London: Academic Pr. p 21–39.

Eggleton RA, Buseck PR. 1980. High-resolution electron microscopy of feldspar weathering. Clays Clay Miner 28: 173–178.

Fitz Gerald JD. 1993. Slowly-cooled, orthoclase-rich alkali feldspars: Microstructures and implications for Ar-Diffusion [abstract]. NATO ASI Series Meet; Edinburgh, Scotland.

Fitz Gerald JD, Harrison TM. 1993. Argon diffusion domains in K-feldspar I: Microstructures in MH-10. Contrib Mineral Petrol 113:367–380.

Fitz Gerald JD, McLaren AC. 1982. The microstructures of microcline from some granitic rocks and pegmatites. Contrib Mineral Petrol 80:219–229.

Gandais M, Williame C. 1984. Mechanical properties of feldspars. In: Brown WL, editor. Feldspars and feldspathoids, NATO ASI Series C 137. Dordrecht: D. Reidel. p 207–246.

Gard JA. 1972. The electron-optical investigation of clays. Mineral Soc Monograph 3 (Clay Miner Group). Oxford: Alden Pr. 383 p.

Goldberg SA, Trupe CH, Adams MG. 1992. Pressure–temperature–time constraints for a segment of the Spruce Pine thrust sheet, North Carolina Blue Ridge [abstract]. Geol Soc Am Abstr with Prog 24:17.

Kohyama N, Fukushima K, Fukami A. 1978. Observation of the hydrated form of tubular halloysite by an electron microscope equipped with an environmental cell. Clays Clay Miner 26:25–40.

McLaren AC. 1978. Defects and microstructures in feldspars. Chem Phys Solids Surf Chem Soc 7:1–30.

Parham WE. 1969. Formation of halloysite from feldspar: Low temperature artificial weathering versus natural weathering. Clays Clay Miner 17:13–22.

Parker JM III. 1949. Geology and structure of part of the Spruce Pine District, North Carolina. NC Dept Conserv and Devel Bull 65. 26 p.

Parsons I, Brown WL. 1984. Feldspars and the thermal history of igneous rocks. NATO ASI Series C137:317–71.

Parsons I. 1993. Fast routes for isotopic exchange in alkali feldspars [abstract]. NATO ASI Series Meet; Edinburgh, Scotland.

Rowe GL, Jr., Brantley SL. 1993. Estimation of the dissolution rates of andesitic glass, plagioclase and pyroxene in a flank aquifer of Poas Volcano, Costa Rica. Chem Geol 105:71–87.

Smith JV, Brown WL. 1988. Feldspar Minerals, vol. 1. New York: Springer-Verlag. 828 p.

Sverdrup HU. 1990. The kinetics of base cation release due to chemical weathering. Sweden: Lund University Pr. 246 p.

Swoboda-Colberg NG, Drever J. 1993. Mineral dissolution rates in plot-scale field and laboratory experiments. Chem Geol 105:51–69.

Tibballs JE, Olsen A. 1977. An electron microscopic study of some twinning and exsolution textures in microcline amazonites. Phys Chem Miner 1:313–324.

Worden RH, Walker FDL, Parsons I, Brown WL. 1990. Development of microporosity diffusion channels and deuteric coarsening in perthitic alkali feldspars. Contrib Mineral Petrol 104:507–515.

Zeitler PK, Fitz Gerald JD. 1986. Saddle-shaped $^{40}Ar/^{39}Ar$ age spectra from young, microstructurally complex potassium feldspars. Geochim Cosmochim Acta 50:1185–1199.

(*Received 4 March 1996; accepted 11 July 1996; Ms. 2750*)